

## OCEANOGRAPHY

# New technology reveals the role of giant larvaceans in oceanic carbon cycling

Kakani Katija,\* Rob E. Sherlock, Alana D. Sherman, Bruce H. Robison

To accurately assess the impacts of climate change on our planet, modeling of oceanic systems and understanding how atmospheric carbon is transported from surface waters to the deep benthos are required. The biological pump drives the transport of carbon through the ocean's depths, and the rates at which carbon is removed and sequestered are often dependent on the grazing abilities of surface and midwater organisms. Some of the most effective and abundant midwater grazers are filter-feeding invertebrates. Although the impact of smaller, near-surface filter feeders is generally known, efforts to quantify the impact of deeper filter feeders, such as giant larvaceans, have been unsuccessful. Giant larvaceans occupy the upper 400 m of the water column, where they build complex mucus filtering structures that reach diameters greater than 1 m. Because of the fragility of these structures, direct measurements of filtration rates require in situ methods. Hence, we developed DeepPIV, an instrument deployed from a remotely operated vehicle that enables the direct measurement of in situ filtration rates. The rates measured for giant larvaceans exceed those of any other zooplankton filter feeder. Given these filtration rates and abundance data from a 22-year time series, the grazing impact of giant larvaceans far exceeds previous estimates, with the potential for processing their 200-m principal depth range in Monterey Bay in as little as 13 days. Technologies such as DeepPIV will enable more accurate assessments of the long-term removal of atmospheric carbon by deep-water biota.

## INTRODUCTION

An essential measurement for modeling oceanic ecosystems is the determination of rates at which phytoplankton and other organic particles are ingested by zooplankton consumers. Grazing rates for copepods and euphausiids have been reliably measured in the laboratory (1, 2), and the filtration rates of gelatinous suspension feeders, such as salps and small larvaceans, have been measured in the field (3, 4). Unfortunately, no feeding rate data exist for a group of enigmatic species whose important contribution to carbon flux in the ocean has only recently become apparent (5). Giant larvaceans, despite their abundance and widespread distribution, pose a significant challenge for making these measurements; to date, there is only an estimate of their feeding rate based on extrapolation from much smaller species (6).

Larvaceans, also known as appendicularians, occur throughout the world's oceans (7–11) and are often found to be second only to copepods in terms of zooplankton abundance (12–14). Larvaceans are tadpole-shaped basal chordates that are pelagic throughout their life cycle (15); their morphology consists of a trunk (or head) and tail (Fig. 1). Rhythmic motion of the tail is used to pump water-borne food particles through a complex mucus filtering structure that is attached to the trunk. This mucus structure is called a “house” because the animal lives inside it (movie S1) (16–18). Small larvaceans, such as those in the genus *Oikopleura*, are widely distributed near the surface of the ocean from subpolar regions to the tropics (3, 19, 20). Laboratory studies have shown that some species can concentrate food particles from 100 to 1000 times the density of natural suspensions outside the house (21), with clearance rates of 100% for some particle size classes (15).

## Giant larvaceans construct elaborate mucus structures to filter food

Most larvacean species are relatively small with total lengths from 2 to 8 mm, living within houses that range from 4 to 38 mm in diameter

(16). Giant larvaceans in the genus *Bathochordaeus* are generally an order of magnitude larger (at 3- to 10-cm total length as adults), and they create large houses that can exceed 1 m in greatest dimension (22, 23). *Bathochordaeus* houses consist of an outer structure that excludes large particles and a fine-mesh inner filter to concentrate particles of the appropriate size for ingestion. The inner filter of a *Bathochordaeus* house has a tail chamber that receives the particle-laden water propelled by the animal's beating tail (Fig. 1). The tail chamber directs water into the two fluted arms of the inner feeding filter, where particles are entrained and carried into the animal's mouth via a buccal tube (23). When its feeding structure becomes clogged, a larvacean discards its mucus house and builds another (24). For smaller species, this can occur on an hourly basis; for giant larvaceans, replacement intervals can be daily (5, 25). Discarded houses are typically rich in nutrients; large ones collapse and sink rapidly to the deep seafloor, circumventing the microbial degradation that mineralizes the organic content of smaller, more slowly sinking detritus (5, 6, 24). Through this process, giant larvaceans contribute significantly to the biological pump and can be regionally responsible for as much as one-third of the carbon flux from near-surface waters to the deep benthos (5).

*Bathochordaeus* has been reported from the North and South Pacific Ocean, the North and South Atlantic Ocean, and the Indian Ocean. Despite their widespread distribution, they are poorly known and the grazing impact of the largest larvaceans has not been quantified. To date, giant larvaceans have proven to be intractable for study in the laboratory. Three species of *Bathochordaeus* can be found in Monterey Bay: *Bathochordaeus stygius*, *Bathochordaeus charon*, and a newly described species with a bright blue tail margin, *Bathochordaeus mcnutti* (26, 27). The fragile nature of *Bathochordaeus*' mucus house, not to mention its great size, is such that they cannot be collected intact by any available means (6). Although numerous living specimens have been collected, none has ever built a functional house in the laboratory. Given these constraints, the only viable prospect for measuring the feeding rates of giant larvaceans while pumping in their houses is to obtain the data in situ.

Research and Development, Monterey Bay Aquarium Research Institute, Moss Landing, CA 95039, USA.

\*Corresponding author. Email: kakani@mbari.org

2017 © The Authors, some rights reserved; exclusive licensee American Association for the Advancement of Science. Distributed under a Creative Commons Attribution NonCommercial License 4.0 (CC BY-NC).

Downloaded from <http://advances.sciencemag.org/> on June 15, 2019

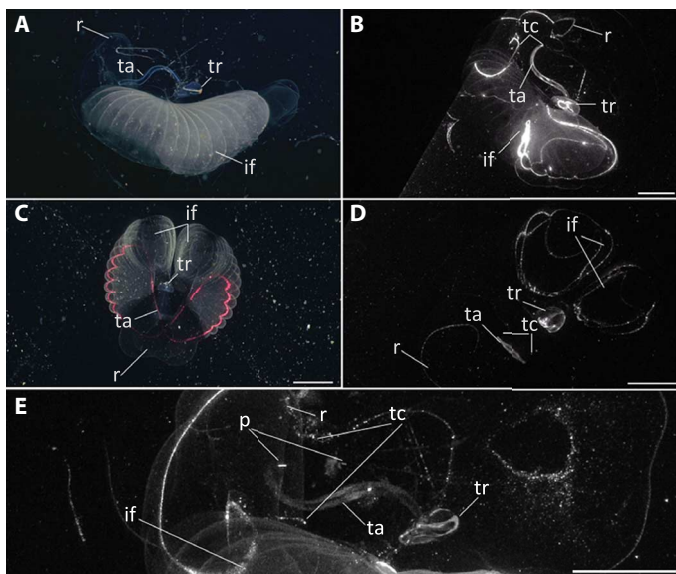


**Fig. 1. Illumination type provides differing views of *Bathochordaeus mcnutti* (top) and *B. stygius* (middle) inner filter structures while revealing internal flow. (A and B) Lateral view. (C and D) Dorsal view. (A and C) LED illumination. (B and D) Planar laser illumination (using DeepPIV). The laser sheet (red light) can also be seen during LED illumination in (C). (E) Lateral view of pumping *B. stygius* with a few particle (p) streaks identified and the upper and lower extent of the tail chamber walls at the entrance to the inner filter/ramp region. ta, tail; tr, trunk; if, inner filter; r, ramp; tc, tail chamber. Scale bars, 3 cm.**

### Novel instrumentation to measure in situ filtration rates

Here, we describe the use of novel instrumentation, deployed by a remotely operated vehicle (ROV), that directly measures the volume flow rates (or filtration rates) of giant larvaceans in situ. Although filtration rates can be considered as clearance rates by assuming 100% retention of particles, here we only present filtration rates because of their relevance in estimating the removal of carbon by filter-feeding larvaceans. By combining these filtration rate measurements with long-term time-series data on the vertical distribution and abundance of *Bathochordaeus*, we can calculate their grazing impact. Two distinct technological challenges were addressed: (i) to develop noninvasive visualization tools that allow for the resolution of internal structures within the filtration system without disrupting the pumping animal, and (ii) to use visualization tools to directly measure fine-scale fluid motion and quantify filtration rates within the house.

Toward this end, engineers at the Monterey Bay Aquarium Research Institute (MBARI) developed DeepPIV, an instrument that allows for the quantitative visualization of fluid motion through particle tracking and particle image velocimetry (PIV) (28, 29). DeepPIV uses a laser sheet coupled to a high-resolution video camera to illuminate and record suspended particles moving in seawater (fig. S1). By mounting the instrument on an ROV trimmed to near-neutral buoyancy, fine control of the vehicle and subsequent positioning of the instrument can be achieved by a pilot aboard a surface vessel (30). With this system, quantitative visualizations of fine-scale fluid motion can be achieved from the sea surface to the maximum depth rating of the ROV.

Conventional ROV lights, either light-emitting diodes (LEDs) or gas-discharge lamps, provide detail on the external surfaces of *Bathochordaeus* houses (Fig. 1, A and C, and movie S1) (22, 23), but

they yield minimal information about their internal structures and processes. Because of the diaphanous nature of the larvacean mucus house, DeepPIV's laser sheet can penetrate to illuminate particle motion within the tail chamber and inside the inner feeding filter (Fig. 1, B and D). This allows for the noninvasive quantification of filtration rates generated by pumping larvaceans within their houses (Fig. 1E and movie S2). In addition, laser sheet illumination provides the necessary contrasting agent to distinguish between the particle-laden, water-filled cavities and the mucoid structures within the larvacean house (Fig. 1, B and D). Thus, ROV deployments with DeepPIV provide a new means to measure filtration rates and small-scale biological fluid interactions while also enabling the description and measurement of complex morphology within gelatinous or mucus structures.

## RESULTS

### ROV-enabled giant larvacean observations

Giant larvaceans were observed from June to December 2015 during cruises on research vessels (RVs) *Western Flyer* and *Rachel Carson* in Monterey Bay, California. DeepPIV was deployed on 13 separate dives affixed to MBARI's *MiniROV* (fig. S1). During these deployments, 71 individuals of the genus *Bathochordaeus* were observed, and flow measurements were collected on 24 individuals. Filtration rates were quantified for seven individual *B. stygius* and three individual *B. mcnutti* for multiple tail pumping cycles (Table 1), using strict criteria for selecting video clips to measure fluid motion within the larvacean house (see Materials and Methods) (31).

### In situ filtration rates of giant larvaceans

DeepPIV measurements of filtration rates were conducted on specimens of *Bathochordaeus* that ranged in trunk length from 0.9 to 2.7 cm (Table 1). The smallest of these (BS7, Table 1) represents the minimum size limit for which flow measurements can be resolved with the current instrumentation. Filtration rates generally increased with larvacean size, which is consistent with laboratory measurements of smaller larvaceans in the genus *Oikopleura* (32, 33). The average filtration rate for giant larvaceans with a trunk length of greater than 1.5 cm was 42.9 liters hour<sup>-1</sup>; maximum filtration rate was 76.2 liters hour<sup>-1</sup> (Table 1). These rate measurements were compared with a biomechanical model for smaller *Oikopleura* species that uses tail morphology and kinematics during pumping to estimate filtration rates (fig. S2) (21). The scaled-up rates from the biomechanical model matched *B. stygius* filtration rates relatively well; however, differences between the *Oikopleura* model and measured rates for *B. mcnutti* differed by nearly a factor of 2 for one individual (BM1, Table 1). These differences may be attributed to variations in tail kinematics between species and/or divergences in tail chamber shape.

The average in situ filtration rates for *Bathochordaeus* reported here are larger by a factor of 4 than the estimated rate in the literature based on extrapolation from oikopleurid larvaceans (6, 21). Differences between previous measurements and our estimates using the same biomechanical model may arise from the higher temporal and spatial resolution of modern ROV camera systems. In addition, the filtration rates of giant larvaceans are at least one and, in some cases, three orders of magnitude greater than those reported for the smaller oikopleurids (18). The maximum filtration rate for *B. mcnutti* (>20 ml s<sup>-1</sup>) exceeds the maximum filtration rates reported for salps (15.3 ml s<sup>-1</sup>), which were previously regarded as the highest rates for any zooplankton filter feeder (34, 35). On the basis of the frequency with

**Table 1. Summary of morphological, kinematic, and filtration performance parameters for in situ filtration measurements of *B. stygius* and *B. mcnutti* using DeepPIV.** Thorough vetting of the DeepPIV measurements yielded filtration results on seven *B. stygius* (BS) and three *B. mcnutti* (BM) individuals. The number of tail-beat cycles per individual is *N*. The tail wave is characterized by amplitude (*a*) and wavelength ( $\lambda$ ) of the tail, and the total area of fluid constrained by the tail is  $A_{tot}$ . Using the tail-beat frequency (*F*) and the tail width (*W*), the biomechanical model volume flow rate ( $Q_{i,model}$ ) can be estimated and compared to the measured value ( $Q_{i,meas}$ ).

	Trunk dimensions			Tail dimensions			Inlet chamber dimensions			Tail wave characteristics		<i>N</i>	<i>F</i> (s <sup>-1</sup> )	Maximum flow rate cm s <sup>-1</sup>	Average flow rate cm s <sup>-1</sup>	Volume flow rate ( $Q_{i,meas}$ ) (cm <sup>3</sup> s <sup>-1</sup> )	Volume flow rate ( $Q_{i,meas}$ ) (liter hour <sup>-1</sup> )
	<i>W</i> (cm)	<i>H</i> (cm)	<i>L</i> (cm)	<i>W</i> (cm)	<i>L</i> (cm)	<i>W</i> (cm)	<i>H</i> (cm)	<i>a</i> (cm)	$\lambda$ (cm)	$A_{tot}$ (cm <sup>2</sup> )							
<b><i>B. stygius</i></b>																	
BS1	1.6	0.9	1.6	2.6	4.5	2.6	2.3	0.9	3.9	2.4	4	1.26 ± 0.03	1.6 ± 0.3	1.0 ± 0.2	6.3 ± 1.3	22.7 ± 4.8	28.2
BS2	1.3	0.9	1.7	2.1	4.8	2.5	2.2	1.1	4.2	3.0	8	1.13 ± 0.04	—	—	—	—	25.8
BS3	1.5	0.9	1.8	2.1	4.7	2.1	2.2	1.2	4.5	3.5	1	0.70	2.4	1.6	7.2	25.8	18.2
BS4	1.8	1.0	1.8	2.3	5.0	2.3	2.2	1.2	4.4	3.5	9	0.72 ± 0.08	2.1 ± 0.4	1.4 ± 0.3	7.1 ± 1.5	25.5 ± 5.4	21.0
BS5	1.1	0.9	1.8	2.2	5.4	2.2	2.3	1.1	4.7	3.3	11	1.01 ± 0.04	2.2 ± 0.4	1.5 ± 0.3	7.5 ± 1.4	26.8 ± 4.9	27.1
BS6	1.4	1.0	1.7	2.1	5.1	2.1	2.5	1.0	4.5	2.9	10	0.97 ± 0.04	2.6 ± 0.2	1.8 ± 0.2	9.5 ± 0.8	34.2 ± 3.0	21.4
BS7	0.5	0.4	0.9	0.8	2.8	0.8	1.4	0.5	2.6	0.9	3	0.40 ± 0.02	1.1 ± 0.2	0.7 ± 0.2	0.8 ± 0.2	2.8 ± 0.6	0.96
<b><i>B. mcnutti</i></b>																	
BM1	2.3	1.3	2.5	3.2	6.1	3.1	2.7	1.4	5.5	5.0	3	0.59 ± 0.02	3.2 ± 0.5	2.2 ± 0.4	18.0 ± 3.0	64.8 ± 10.8	34.0
BM2	2.4	1.4	2.7	3.1	6.6	3.1	2.9	2.0	5.2	7.0	5	0.68 ± 0.05	3.5 ± 1.0	2.4 ± 0.7	21.2 ± 6.3	76.2 ± 22.8	53.1
BM3	1.9	1.0	2.4	2.7	5.8	2.7	2.5	1.7	5.2	5.7	2	1.04 ± 0.09	3.8 ± 2.0	2.6 ± 1.4	17.5 ± 9.3	67.2 ± 29.2	57.7

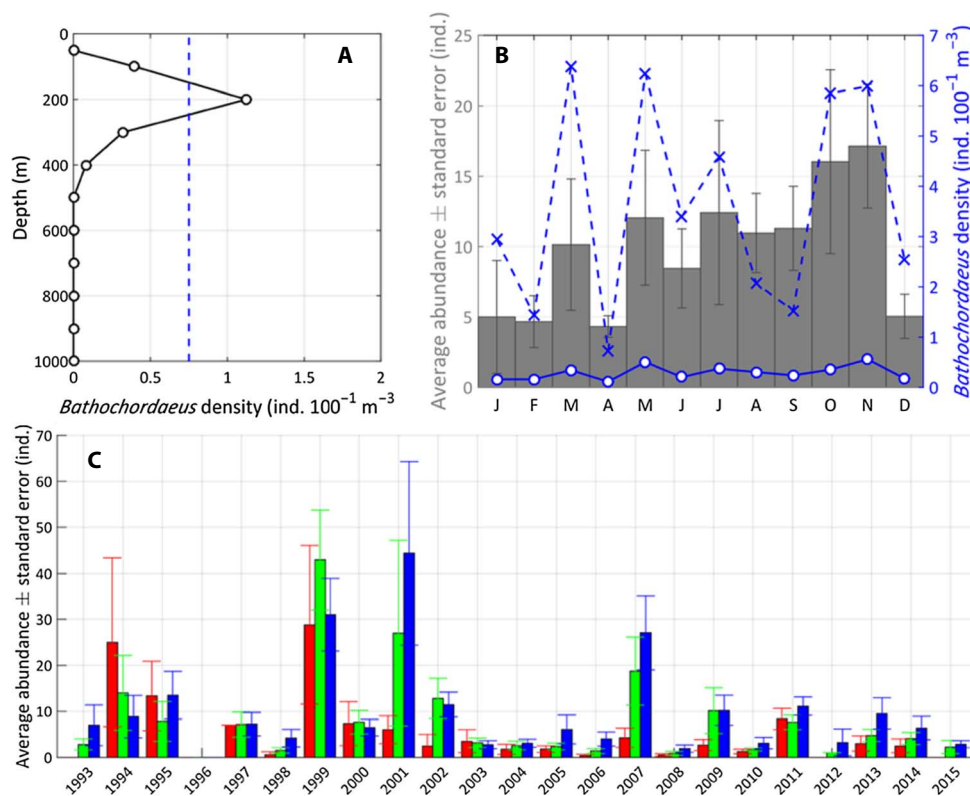


**Fig. 2. ROV-collected video transect data for all counts of the genus *Bathochordaeus* at MW1 in Monterey Bay from 1993 to 2015.** (A) Representative data set showing larvacean density with depth during a single series of video transects. Averaged density between 100 and 300 m is indicated by the blue dashed line. (B) Average abundance with SE (gray bars, left vertical axis) and average (open circles, blue solid line) and maximum (hatches, blue dashed line) *Bathochordaeus* densities binned by month. (C) Average abundance of *Bathochordaeus* during spring (red), upwelling (green), and winter (blue) seasons; error bars indicate the SE binned by season and year.

which giant larvaceans were actively pumping when we first encountered them with the ROV, and long-duration observations during DeepPIV measurements, we estimate that they are filtering ambient seawater about 66% of the time.

### Long-term abundance and densities of giant larvaceans in Monterey Bay

To calculate the overall grazing impact of giant larvaceans in Monterey Bay, we quantified their long-term abundance and densities using MBARI's unique mesopelagic time-series database. These data have been generated during quantitative ROV video transects at Midwater Station 1 (MW1: 36°42'N, 122°02'W) on a monthly to bimonthly basis since 1993 (5). Data on *Bathochordaeus* abundance, density, and vertical distribution (Fig. 2) were extracted from the time-series database using MBARI's Video Annotation and Reference System (VARS) (36).

Our time-series data reveal distinct trends in the spatiotemporal characteristics of giant larvaceans in Monterey Bay. Occupied *Bathochordaeus* houses are mostly restricted to the upper 400 m of the water column, with peak abundance generally between 100 and 300 m (Fig. 2A) (5). High overall abundance usually occurs during and shortly after the local upwelling season and then decreases by the end of winter (Fig. 2, B and C). Densities between 100 and 300 m averaged 0.29 individuals  $100^{-1} \text{ m}^{-3}$  between 1993 and 2015, with maximum densities as high as 6.38 individuals  $100^{-1} \text{ m}^{-3}$ . Densities as high as 12.10 individuals  $100^{-1} \text{ m}^{-3}$  were recorded at depths above 100 m, but these instances were not common.

### DISCUSSION

To quantify the impact of grazing by giant larvaceans in the upper water column they inhabit, we can use their average and maximum densities, along with their average and maximum filtration rates to calculate impact. Within their principal depth range of 100 to 300 m, at average density and average filtration rate, their portion of the water column in Monterey Bay will be completely grazed within 500 days. At peak density and maximum filtration rate, the same volume of water will be filtered in as little as 13 days. Given that the maximum abundance of *Bathochordaeus* in Monterey Bay coincides with the upwelling-driven seasonal peak in primary production (37), actual grazing impact is likely shifted toward the high end of this range. Because ingested particles are rendered into fecal pellets, and a discarded house with its burden of large particles becomes a rapidly descending "sinker" (5), the net result of giant larvacean grazing is the acceleration of particulate organic matter out of the upper water column.

Although our estimates of grazing impact by giant larvaceans in Monterey Bay are based on a data set collected at a single oceanographic station, no comparable oceanic data set of long-term abundance and filtration rates exists. Our calculations of overall impact are conservative because they include only those individuals found between 100 and 300 m and necessarily exclude the filtration impact by more numerous, smaller oikopleurid species. Nevertheless, our results reveal a much greater contribution to vertical carbon flux by giant larvaceans than was predicted from the limited indirect data on their filtration rates that

were previously available. Further investigation of midwater filter feeders, enabled by technologies that characterize animal-fluid interactions in situ, will lead to more accurate assessments of the role of the deep-water biota in the long-term removal of carbon from the atmosphere.

## MATERIALS AND METHODS

### Measuring in situ filtration rates and morphology

To quantify the filtration impact of giant larvaceans in situ, we developed DeepPIV, an instrument that allows for the measurement of fine-scale fluid motions that is similar in concept to previous technologies deployed in rivers and shallow ocean depths (31, 38–40). Unlike earlier versions of this technology, DeepPIV can be deployed from ROVs that are capable of diving to depths where giant larvaceans and other midwater organisms are found (22, 23).

DeepPIV consists of a laser housing deployed via a rigid arm that attaches to an ROV (fig. S1). Within the laser housing is a continuous, 1-W, 671-nm laser (Laserglow Technologies) and line-generating optics (Edmund Optics) that illuminate a sheet of light approximately 1 mm thick in front of the ROV science camera (FCB-EV7100; Sony Corporation). The laser sheet plane is approximately 50 cm in front of the camera dome, and the laser sheet optics can illuminate an area as large as 20 cm × 20 cm in front of the camera. The ROV science camera records high-definition (1920 pixel × 1080 pixel), progressive format video at 60 frames per second, and the camera housing and optics (Mini Zeus II; Insite Pacific Incorporated) are specially designed to minimize image distortion. The science camera has a 10× optical zoom, allowing for image fields of view ranging in size from 13 cm × 7 cm to 165 cm × 90 cm while focused on the laser sheet. The videos were recorded on external drives (AJA Video Systems) using the camera's high-definition multimedia interface output and stored for further data analysis.

Giant larvaceans were observed from June to December 2015 using DeepPIV (mounted to *MiniROV*; fig. S1) during cruises aboard the RVs *Western Flyer* and *Rachel Carson*. During 13 separate deployments of the instrument, we observed 71 individuals of the genus *Bathochordaeus* (specifically *B. stygius* and blue-tailed *Bathochordaeus*) and collected DeepPIV measurements on 24 individuals, resulting in nearly 49 hours of high-definition video. Criteria for selecting clips to measure particle streak length included the following: (i) limited ROV motion, (ii) accurate positioning of the laser sheet with respect to the organism (that is, the pumping tail and trunk needed to be bisected by a 1-mm-thick laser sheet), and (iii) conditions (i) and (ii) were met for at least a single pumping cycle of the tail. These are similar criteria used by other studies conducting in situ fluid motion measurements induced by swimming zooplankton (31, 41). Movie S1 shows an example video clip (for BS5, Table 1), where the larvacean undergoes more than six tail-beat cycles.

Although DeepPIV was originally developed to conduct in situ PIV measurements (28, 29), this analysis technique was not used because of limited particle densities and laser power. Instead, we used the length of particle streaks as a measure of fluid motion, which has been used in previous measurements with gelatinous zooplankton (34). Hence, particle streak length within the tail chamber and near the inlet of the inner filter was used to directly measure the flow rate into the inner filter. In addition, the laser sheet illumination provided by DeepPIV can reveal morphology within the mucus house to measure the inlet and tail chamber size (see Fig. 1E). These two quantities can be combined to directly measure filtration rates of giant larvaceans.

Particle streak lengths were measured through the entrance plane of the inner filter, which was near the posterior end of the tail, and are indicated by the tail chamber lines in Fig. 1E. The number of particles measured per frame varied from 1 to 10 particles for the duration of the tail-beat cycle. For each frame, the maximum length of particle streaks was recorded and assumed to represent the centerline velocity within the entrance of the inner filter. An average centerline velocity ( $U_{\max}$ ) through the tail-beat cycle can be found by averaging the maximum velocity measured for each frame. Using equations for Poiseuille flow (42), the velocity profile within the tail chamber exit can be calculated using

$$u = -\frac{1}{4\mu} \frac{dp}{dr} (r_0^2 - r^2) \quad (1)$$

where  $\mu$  is the dynamic viscosity of seawater ( $1.08 \times 10^{-3}$  Pa·s for seawater at 20°C),  $r_0$  is the maximum radius of the tail chamber, and, for a laminar flow

$$\frac{dp}{dr} = -4\mu \frac{U_{\max}}{r^2}$$

Integrating the velocity profile ( $u$ ) in Eq. 1 across the tail chamber will give the average flow rate over the tail-beat cycle into the inner filter of the larvacean house.

Determining the size of the organism and its mucus house morphology was conducted by using sizing lasers or by placing an object of known size (for example, the laser housing) in the field of view of the science camera and laser sheet. Therefore, using the measured dimensions of the inlet and tail chamber, a cross-sectional area can be found within the tail chamber, and filtration rate can be obtained by multiplying the cross-sectional area by the average flow rate into the inner filter.

### Estimating in situ filtration rates using a biomechanical model

In situ measurements of filtration rate using DeepPIV were compared with a scaled-up biomechanical model that has been used to estimate the filtration rate of smaller larvaceans (21). This model is based on morphological (tail width,  $W$ ) and kinematics parameters (tail beat frequency,  $F$ ) of the pumping larvacean within its house. The biomechanical model assumes that all fluid that enters the inner filter structure of a larvacean house is bounded between the tail and tail chamber (fig. S2), and the volume of fluid that enters the inner filter can be determined by measuring the bounded area during a single swimming cycle (or  $A_{\text{tot}}$ ; fig. S2, gray shaded area). The area bounded by the tail during a single swimming cycle can be estimated by characterizing the wave that travels along the tail during pumping, where  $A$  is the amplitude of the wave and  $\lambda$  is its wavelength. Assuming that the total area bound by the tail in the tail chamber is twice the area under the parabolic shape of the tail, or  $A_{\text{tot}} = \frac{2}{3}A\lambda$ , the volume flow rate through the tail chamber and into the inner filter (or filtration rate) is

$$Q_i = W \cdot F \cdot A_{\text{tot}} = \frac{2}{3} W \cdot F \cdot A\lambda \quad (2)$$

### Conducting ROV video transects to estimate larvacean density

Quantitative, mesopelagic video transects have been conducted at MW1 in Monterey Bay from 1993 to present. The MW1 site (36°42'N,

122°02'W) is located over the axis of the Monterey Submarine Canyon, where the water column depth is approximately 1600 m. Depth declines rapidly to the west of this time-series station, and the area is open to oceanic water. Transects start at a depth of 50 m and continue in 100-m increments from 100 to 1000 m. Transect dives are made approximately once each month, and the efficacy of this system is well documented (5).

Vertical distribution and abundance measurements for the meso-pelagic time series were made with three similarly equipped ROVs: *Ventana* (1993 to present), an electrohydraulic Hysub 40 outfitted for scientific research; *Tiburón* (2000–2008), an electric vehicle; and *Doc Ricketts* (2010 to present), an electrohydraulic vehicle. For transecting, the ROV lights were arranged to give broad forward coverage, the camera lens was always set to its widest angle, and focus was adjusted to give the largest depth of field from 1 to 4 m in front of the vehicle. Video images were transmitted through optical fibers in the ROV's tether and were recorded on standard- or high-definition tapes aboard the surface support ship.

The video equipment on MBARI's ROVs has changed over time as video technology has improved. Four principal broadcast-quality cameras have been used: a standard-definition (720-pixel × 480-pixel resolution) Sony 3-chip (*Ventana*, 1993–1999) and Panasonic 3-chip (*Tiburón*, 1996–2005), a high-definition (1920-pixel × 1080-pixel resolution) Sony HDTV (*Ventana*, 1999–2007), and Ikegami HDL-40 (*Ventana*, 2007 to present; *Tiburón*, 2005–2007; and *Doc Ricketts*, 2009 to present). Because equipment and resolution have changed, the swept area has varied from 2.43 to 5.96 m<sup>2</sup> (currently 3.8 and 4.0 m<sup>2</sup> for *Ventana* and *Doc Ricketts*, respectively), and these numbers were used to calculate transect volumes. During transects, the ROV was piloted at a mean speed of 0.5 m s<sup>-1</sup>, just slow enough for the moving video images to remain sharp. Transects were conducted at constant depth for 10 min. Mean transect length was 324 m (SD ± 52 m), which was measured in real time by an acoustic current meter (Falmouth Scientific), and mean transect volumes were approximately 1450 m<sup>3</sup>.

At the completion of each transect series, counts of individual organisms observed for every five frames of video were manually entered into MBARI's VARS (35). Using the searchable VARS software interface, all counts of a given annotation can be compiled and organized with respect to time, depth, and other parameters. We searched for instances of *Bathochordaeus*, which includes results for *B. stygius*, *B. charon*, and *B. mcnutti*, and VARS returned 2670 counts or individuals between 1997 and 2016. The depth-specific density of giant larvaceans based on the average (between 100 and 300 m) and maximum number of individuals ( $\rho_{\text{ave}}$  and  $\rho_{\text{max}}$ , respectively) is determined by dividing the number of individuals at each transect depth by the corresponding transect volume.

### Estimating large-scale filtration impact of giant larvaceans

Using the measured filtration rates (see Table 1) and transect data (see Fig. 2), we can estimate the large-scale filtration and grazing impact of giant larvaceans near MW1 in Monterey Bay, California. Our measurements yielded an average ( $FR_{\text{ave}}$ , 42.9 liters hour<sup>-1</sup>) and maximum filtration rate ( $FR_{\text{max}}$ , 76.2 liters hour<sup>-1</sup>) for individuals in the same size class (excluding BS7 from Table 1). Because the long-term behaviors of both *B. stygius* and *B. mcnutti* are not known, we estimated the relative time spent filtering (or pumping frequency,  $\eta$ ) by (i) using the VARS database to randomly select 200 individuals to determine whether they were pumping upon first observation by the ROV and (ii) directly measuring pumping frequency during more than 5 hours of DeepPIV measurements and observations of the 10 individuals re-

ported here. Method 1 was similar to previous efforts that quantified pumping frequency of smaller larvaceans (3, 19) and yielded a pumping frequency of 40% for *Bathochordaeus*; method 2 yielded an average pumping frequency of 92%. Because we are unable to determine what effect, if any, the presence of the ROV has on larvacean pumping behavior, we averaged the two results to estimate a pumping frequency of 66% for *Bathochordaeus*.

To determine the number of individuals of the genus *Bathochordaeus* that were present in the transected volume at MW1, we used the average and maximum densities ( $\rho_{\text{ave}}$  and  $\rho_{\text{max}}$ , respectively) of individuals determined from the video transect data. For each video transect, the camera properties (for example, field-of-view area and video aspect ratio) and distances traveled during measurements at each depth were recorded. Averaging these quantities for each video transect conducted between 1993 and 2015 yielded an average field-of-view area ( $A_{\text{FOV}}$ ) of 4.42 m<sup>2</sup>, transect volume ( $V$ ) of 1495 m<sup>3</sup>, and distance traveled during a transect ( $d$ ) of 338 m. Given the average aspect ratio of the science camera used during transect records, the width of the recorded area ( $x$ ) was 2.74 m. Using these quantities, and noting that individuals of the genus *Bathochordaeus* are predominantly found between 100 and 300 m, the total volume of water in the video transect region ( $V_{\text{tot}}$ ) is  $V_{\text{tot}} = 200xd$  or  $1.85 \times 10^5$  m<sup>3</sup>.

The total number of individuals based on  $\rho_{\text{ave}}$  and  $\rho_{\text{max}}$  (or  $N_{\text{ave}}$  and  $N_{\text{max}}$ ) is found by multiplying their respective densities by  $V_{\text{tot}}$  and is 545 and  $1.18 \times 10^4$ , respectively. The number of days ( $D$ ) it would take for a population of *Bathochordaeus* to graze between 100- and 300-m depths of the transect volume at MW1 can be found by

$$D_{\text{ave,max}} = \frac{1}{24} \frac{V_{\text{tot}}}{\eta FR_{\text{ave,max}} N_{\text{ave,max}}} \quad (3)$$

where 24 is the conversion factor from hours to days, and the “ave” and “max” terms can be used interchangeably. Therefore, it would take anywhere from 13 days (using  $N_{\text{max}}$  and  $FR_{\text{max}}$ ) to 500 days (using  $N_{\text{ave}}$  and  $FR_{\text{ave}}$ ) to completely filter the volume  $V_{\text{tot}}$  between 100 and 300 m in Monterey Bay.

### SUPPLEMENTARY MATERIALS

Supplementary material for this article is available at <http://advances.sciencemag.org/cgi/content/full/3/5/e1602374/DC1>

fig. S1. Filtration rates are quantified using DeepPIV coupled to MBARI's *MiniROV*.

fig. S2. Filtration rates can be estimated using biomechanical considerations.

movie S1. Video collected by MBARI's *MiniROV* science camera while using white LED lights to visualize *B. stygius* feeding in midwater.

movie S2. Video collected by MBARI's *MiniROV* science camera while using the DeepPIV instrumentation reveals how the beating tail of *B. stygius* generates a feeding current inside the inner filter.

### REFERENCES AND NOTES

- G.-A. Paffenhöfer, Grazing and ingestion rates of nauplii, copepodids and adults of the marine planktonic copepod *Calanus helgolandicus*. *Mar. Biol.* **11**, 286–298 (1971).
- L. Dilling, J. Wilson, D. Steinberg, A. L. Alldredge, Feeding by the euphausiid *Euphausia pacifica* and the copepod *Calanus pacificus* on marine snow. *Mar. Ecol. Prog. Ser.* **170**, 189–201 (1998).
- A. L. Alldredge, The impact of appendicularian grazing on natural food concentrations in situ. *Limnol. Oceanogr.* **26**, 247–257 (1981).
- K. R. Sutherland, L. P. Madin, A comparison of filtration rates among pelagic tunicates using kinematic measurements. *Mar. Biol.* **157**, 755–764 (2010).
- B. H. Robison, K. R. Reisenbichler, R. E. Sherlock, Giant larvacean houses: Rapid carbon transport to the deep sea floor. *Science* **308**, 1609–1611 (2005).

6. M. W. Silver, S. L. Coale, C. H. Pilskaln, D. R. Steinberg, Giant aggregates: Importance as microbial centers and agents of material flux in the mesopelagic zone. *Limnol. Oceanogr.* **43**, 498–507 (1998).
7. S.-i. Uye, S. Ichino, Seasonal variations in abundance, size composition, biomass and production rate of *Oikopleura dioica* (Fol) (Tunicata: Appendicularia) in a temperate eutrophic inlet. *J. Exp. Mar. Biol. Ecol.* **189**, 1–11 (1995).
8. R. Fenaux, Q. Bone, D. Deibel, in *The Biology of Pelagic Tunicates* (Oxford Univ. Press, 1998), pp. 251–264.
9. Á. López-Urrutia, R. Harris, J. Acuna, U. Baamstedt, H. J. Fyhn, P. Flood, B. Gasser, G. I. X. Gorsky, M. Martinussen, in *Response of Marine Ecosystems to Global Change: Ecological Impact of Appendicularians*, G. Gorsky, M. J. Youngbluth, D. Deibel, Eds. (Contemporary Publishing International, 2005), pp. 255–276.
10. R. D. Scheinberg, M. R. Landry, A. Calbet, Grazing of two common appendicularians on the natural prey assemblage of a tropical coastal ecosystem. *Mar. Ecol. Prog. Ser.* **294**, 201–212 (2005).
11. C. Jaspers, T. G. Nielsen, J. Carstensen, R. R. Hopcroft, E. F. Møller, Metazooplankton distribution across the Southern Indian Ocean with emphasis on the role of Larvaceans. *J. Plankton Res.* **31**, 525–540 (2009).
12. R. R. Hopcroft, J. C. Roff, Production of tropical larvaceans in Kingston Harbour, Jamaica: Are we ignoring an important secondary producer? *J. Plankton Res.* **20**, 557–569 (1998).
13. M. R. Landry, W. K. Peterson, V. L. Fagerness, Mesozooplankton grazing in the Southern California Bight. I. Population abundances and gut pigment contents. *Mar. Ecol. Prog. Ser.* **115**, 55–71 (1994).
14. G. Gorsky, R. Fenaux, in *The Biology of Pelagic Tunicates* (Oxford Univ. Press, 1998), pp. 161–169.
15. R. Fenaux, in *The Biology of Pelagic Tunicates* (Oxford Univ. Press, 1998), pp. 151–159.
16. A. L. Alldredge, House morphology and mechanisms of feeding in the Oikopleuridae (Tunicata, Appendicularia). *J. Zool.* **181**, 175–188 (1977).
17. D. Deibel, Feeding mechanism and house of the appendicularian *Oikopleura vanhoffeni*. *Mar. Biol.* **93**, 429–436 (1986).
18. P. R. Flood, Architecture of, and water circulation and flow rate in, the house of the planktonic tunicate *Oikopleura labradoriensis*. *Mar. Biol.* **111**, 95–111 (1991).
19. D. Deibel, Filter feeding by *Oikopleura vanhoffeni*: Grazing impact on suspended particles in cold ocean waters. *Mar. Biol.* **99**, 177–186 (1988).
20. R. Sato, Y. Ishibashi, Y. Tanaka, T. Ishimaru, M. J. Dagg, Productivity and grazing impact of *Oikopleura dioica* (Tunicata, Appendicularia) in Tokyo Bay. *J. Plankton Res.* **30**, 299–309 (2007).
21. C. C. Morris, D. Deibel, Flow rate and particle concentration within the house of the pelagic tunicate *Oikopleura vanhoffeni*. *Mar. Biol.* **115**, 445–452 (1993).
22. E. G. Barham, Giant larvacean houses: Observations from deep submersibles. *Science* **205**, 1129–1131 (1979).
23. W. M. Hamner, B. H. Robison, In situ observations of giant appendicularians in Monterey Bay. *Deep Sea Res. A* **39**, 1299–1313 (1992).
24. A. L. Alldredge, Abandoned larvacean houses: A unique food source in the pelagic environment. *Science* **177**, 885–887 (1972).
25. R. Sato, Y. Tanaka, T. Ishimaru, House production by *Oikopleura dioica* (Tunicata, Appendicularia) under laboratory conditions. *J. Plankton Res.* **23**, 415–423 (2001).
26. R. E. Sherlock, K. R. Walz, B. H. Robison, The first definitive record of the giant larvacean, *Bathochordaeus charon*, since its original description in 1900 and a range extension to the northeast Pacific Ocean. *Mar. Biodivers. Rec.* **9**, 79 (2016).
27. R. E. Sherlock, K. R. Walz, K. L. Schlining, B. H. Robison, Morphology, ecology, and molecular biology of a new species of giant larvacean in the Eastern North Pacific: *Bathochordaeus mcnutti* sp. nov. *Mar. Biol.* **164**, 20 (2017).
28. R. Adrian, Particle-imaging techniques for experimental fluid-mechanics. *Annu. Rev. Fluid Mech.* **23**, 261–304 (1991).
29. C. E. Willert, M. Gharib, Digital particle image velocimetry. *Exp. Fluids* **10**, 181–193 (1991).
30. B. H. Robison, The coevolution of undersea vehicles and deep-sea research. *Mar. Technol. Soc. J.* **33**, 65–73 (1999).
31. K. Katija, S. P. Colin, J. H. Costello, J. O. Dabiri, Quantitatively measuring in situ flows using a self-contained underwater velocimetry apparatus (SCUVA). *J. Vis. Exp.* **31**, e2615 (2011).
32. R. Sato, Y. Tanaka, T. Ishimaru, in *Response of Marine Ecosystems to Global Change: Ecological Impact of Appendicularians*, G. Gorsky, M. J. Youngbluth, D. Deibel, Eds. (Contemporary Publishing International, 2005), pp. 189–205.
33. F. Lombard, A. Sciandra, G. Gorsky, Influence of body mass, food concentration, temperature and filtering activity on the oxygen uptake of the appendicularian *Oikopleura dioica*. *Mar. Ecol. Prog. Ser.* **301**, 149–158 (2005).
34. K. R. Sutherland, L. P. Madin, R. Stocker, Filtration of submicrometer particles by pelagic tunicates. *Proc. Natl. Acad. Sci. U.S.A.* **107**, 15129–15134 (2010).
35. L. P. Madin, D. Deibel, in *The Biology of Pelagic Tunicates*, Q. Bone, Ed. (Oxford Univ. Press, 1998), pp. 81–103.
36. B. M. Schlining, N. J. Stout, *MBARI's Video Annotation and Reference System* (IEEE, 2006), pp. 1–5.
37. J. T. Pennington, F. P. Chavez, Seasonal fluctuations of temperature, salinity, nitrate, chlorophyll and primary production at station H3/M1 over 1989–1996 in Monterey Bay, California. *Deep Sea Res. II* **47**, 947–973 (2000).
38. H. M. Tritico, A. J. Cotel, J. N. Clarke, Development, testing and demonstration of a portable submersible miniature particle imaging velocimetry device. *Meas. Sci. Technol.* **18**, 2555–2562 (2007).
39. K. Katija, J. O. Dabiri, In situ field measurements of aquatic animal-fluid interactions using a Self-Contained Underwater Velocimetry Apparatus (SCUVA). *Limnol. Oceanogr. Methods* **6**, 162–171 (2008).
40. B. Wang, Q. Liao, H. A. Bootsma, P.-F. Wang, A dual-beam dual-camera method for a battery-powered underwater miniature PIV (UWMPIV) system. *Exp. Fluids* **52**, 1401–1414 (2012).
41. K. Katija, W. T. Beaulieu, C. Regula, S. P. Colin, J. H. Costello, J. O. Dabiri, Quantification of flows generated by the hydromedusa *Aequorea victoria*: A Lagrangian coherent structure analysis. *Mar. Ecol. Prog. Ser.* **435**, 111–123 (2011).
42. F. M. White, *Viscous Fluid Flow* (McGraw-Hill, 1979).

**Acknowledgments:** We are grateful for the engineering contributions made by D. Graves, C. Kecy, D. Klimov, J. Erickson, and technical staff to the development of DeepPIV. We would also like to thank S. von Thun and K. Schlining for assistance with VARS, the crews of RVs *Rachel Carson* and *Western Flyer*, and the pilots of ROVs *Doc Ricketts*, *Ventana*, and *MiniROV* for their contributions to this project. **Funding:** This work was supported by the David and Lucile Packard Foundation. **Author contributions:** K.K., A.D.S., and B.H.R. designed the study. K.K. performed the experiments, analyzed flow data, and wrote the manuscript. K.K. and R.E.S. extracted and analyzed data from MBARI's VARS database. K.K., A.D.S., R.E.S., and B.H.R. revised the manuscript in its current form. **Competing interests:** B.H.R. was a Research Division Chair at MBARI from 2011 to 2015. The other authors declare that they have no competing interests. **Data and materials availability:** The data used in this manuscript have been archived, and videos used for analysis can be searched using MBARI's VARS ([www.mbari.org/products/research-software/video-annotation-and-reference-system-vars/](http://www.mbari.org/products/research-software/video-annotation-and-reference-system-vars/)). All data needed to evaluate the conclusions in the paper are present in the paper and/or the Supplementary Materials. Additional data related to this paper may be requested from the authors.

Submitted 27 September 2016

Accepted 8 March 2017

Published 3 May 2017

10.1126/sciadv.1602374

**Citation:** K. Katija, R. E. Sherlock, A. D. Sherman, B. H. Robison, New technology reveals the role of giant larvaceans in oceanic carbon cycling. *Sci. Adv.* **3**, e1602374 (2017).

## New technology reveals the role of giant larvaceans in oceanic carbon cycling

Kakani Katija, Rob E. Sherlock, Alana D. Sherman and Bruce H. Robison

*Sci Adv* 3 (5), e1602374.

DOI: 10.1126/sciadv.1602374

### ARTICLE TOOLS

<http://advances.sciencemag.org/content/3/5/e1602374>

### SUPPLEMENTARY MATERIALS

<http://advances.sciencemag.org/content/suppl/2017/05/01/3.5.e1602374.DC1>

### REFERENCES

This article cites 34 articles, 4 of which you can access for free  
<http://advances.sciencemag.org/content/3/5/e1602374#BIBL>

### PERMISSIONS

<http://www.sciencemag.org/help/reprints-and-permissions>

Use of this article is subject to the [Terms of Service](#)

---

*Science Advances* (ISSN 2375-2548) is published by the American Association for the Advancement of Science, 1200 New York Avenue NW, Washington, DC 20005. 2017 © The Authors, some rights reserved; exclusive licensee American Association for the Advancement of Science. No claim to original U.S. Government Works. The title *Science Advances* is a registered trademark of AAAS.